New BIOTECHNOLOGY 70 (2022) 57–66

Contents lists available at ScienceDirect

New BIOTECHNOLOGY

journal homepage: www.elsevier.com/locate/nbt

A unique class I polyhydroxyalkanoate synthase (PhaC) from *Brevundimonas* sp. KH11J01 exists as a functional trimer: A comparative study with PhaC from *Cupriavidus necator* H16

Netsanet Gizaw Assefa *, Hilde Hansen, Bjørn Altermark

Department of Chemistry, Faculty of Natural Sciences and Technology, UIT The Arctic University of Norway, Tromsø, Norway

ARTICLE INFO

Keywords:
Bioplastic
Polyhydroxyalkanoate
PHA synthase
Protein oligomerization
Brevundimonas sp.
Cupriavidus necator H16

ABSTRACT

Polyhydroxyalkanoates (PHAs) are natural biodegradable polyesters that are produced by numerous prokaryotic microorganisms primarily as a carbon- and energy reserve. The PhaC enzyme catalyzes the last step in the PHA biosynthesis pathway and synthesizes PHA polymers from hydroxyalkanoic acids. A type I PhaC from a PHA-producing marine bacterium *Brevundimonas* sp. KH11J01 (BrPhaC) was identified, produced recombinantly and characterized. Its properties were compared with its homolog from *C. necator* H16 (RePhaC). Unlike other PhaCs, it was found that BrPhaC is a lag-phase free enzyme organized as a trimer, even without the presence of a substrate. The enzymatic reaction is initiated instantly irrespective of temperature, in contrast to RePhaC in which the duration of the lag-phase was highly affected by temperature. At 10 °C BrPhaC was 40% active whereas RePhaC was barely active. The significance of using marine microorganisms, harboring cold-active PHA biosynthesis enzymes, for energy efficient PHA production, is also discussed briefly. The unique trimeric organization of BrPhaC challenges our understanding of the PhaC reaction mechanisms, which is mainly based on the crystal structures of the inactive forms of the enzyme.

Introduction

Polyhydroxyalkanoates (PHAs) are promising biodegradable bioplastics which possess biophysical properties comparable to those of conventional plastics [1]. They are natural polyesters produced by a wide range of prokaryotic microorganisms. When the environment these bacteria are dwelling in is challenged by a scarcity of essential nutrients for growth, but with an excess of carbon sources, they tend to accumulate PHA into water-insoluble granules inside the cell. These granules serve as carbon reserves which can later be degraded and consumed by the bacterium when carbon sources become limited in the surrounding environment [2]. The PHA granules additionally provide microorganisms enhanced stress survival and robustness [3,4]. Different types of bacteria can synthesize slightly different PHA building blocks, which at the end determine the characteristics of the bioplastic with respect to elasticity and strength [5–7]. The type of PHA produced is dictated by a set of catalytic enzymes and the types of carbon source in the growth medium [8].

The PHA biosynthetic pathways comprise various steps and involve different enzymes, which produce PHA polymers from hydroxyalkanoic acids [1]. The PHA synthase (PhaC) (EC 2.3.1.304) catalyzes the last step in the pathway. It synthesizes PHA polymers from coenzyme A (CoA) thioesters of the hydroxyalkanoic acids, with concomitant release of the CoA moiety. PHA synthases can be classified into four classes based on their primary structure, subunit composition and substrate specificity [9]. Except Class II synthases, which tend to use medium chain length (MCL) monomers, Classes I, III and IV synthases prefer short chain length (SCL) monomers. New types of PhaCs not belonging to any of the established four classes have been identified recently [10]. PHA heteropolymers composed of mixtures of SCL and MCL monomers appear to possess better thermal and physical properties than homopolymers of SCL or MCL [11]. In that sense, protein engineering of PhaC

Abbreviations: PHA, polyhydroxyalkanoate; PhaC, PHA synthase; BrPhaC, PhaC from Brevundimonas sp.; RePhaC, PhaC from *Cupriavidus necator* H16 (in house construct); CnPhaC, PhaC from *C. necator* H16 (from literature); SCL, Short Chain Length; MCL, Medium Chain Length; ChPhaC, *Chromobacterium* sp. USM2; CcPhaC, PhaC from *Caulobacter crecentus*; RsPhaC, *Rhodovulum sulfidophilum*; TEV, Tobacco Etch Virus; SEC, Size Exclusion Chromatography; DTNB, 5,5'-dithiobis-2-nitrobenzoate; DSC, Differential Scanning Calorimetry; 3HBCoA, 3-Hydroxybutryl Coenzyme A.

* Corresponding author.
E-mail address: netsanet.g.assefa@uit.no (N.G. Assefa).

https://doi.org/10.1016/j.nbt.2022.05.003
Received 17 February 2022; Received in revised form 25 March 2022; Accepted 4 May 2022
Available online 6 May 2022

with the aim of broadening its substrate specificity has become an attractive and appealing approach [1,12]. To achieve this goal, it is important to study the properties of different PhaCs and unravel the enzymatic mechanisms behind the PHA polymerization.

The crystal structures of the catalytic domain of PhaC from the two beta proteobacteria *C. necator* H16 (CnPhaC) [13,14] and *Chromobacterium sp.* USM2 (ChPhaC) [15] have been determined, and recently the co-crystal structure of the catalytic domain of ChPhaC in complex with free CoA also became available [16]. These crystal structures have thrown some light onto the mostly non-understood catalytic and oligomer formation mechanisms. Two mechanisms of catalysis have been proposed in the context of PhaC dimerization [15,16].

In this study, a functional PhaC from the marine alpha proteobacterium *Brevundimonas* sp. KH11J01, isolated from the Arctic environment, with a unique stable trimeric organization in comparison with its well-studied PhaC homolog from *C. necator* H16 (previously called *Ralstonia eutropha* H16, *Wautersia eutropha and Alcaligenes eutrophus*), is presented. A special focus has been given to their differences related to oligomerization patterns and to their thermal adaptation properties. The implication of the results with respect to reduction of cost related to PHA production is discussed briefly.

Materials and methods

Sequence analysis

In addition to PhaC from *Brevundimonas* sp. KH11J01, PhaC protein sequences belonging to *C. necator* H16, *Chromobacterium* sp. USM2, *Rhodovulum sulfidophilum* DSM1374 and *Caulobacter crecentus* NA1000 were downloaded from GenBank. The online program T-coffee [17] was used to align the sequences and EsPript [18] was used to visualize the alignment and the secondary structures. Secondary structures of the catalytic domains belonging to CnPhaC and ChPhaC were extracted from the Protein Data Bank. The secondary structures belonging to the other sequences and the N-terminal domains were predicted using PsiPred [19]. The alignment was manually corrected in the N-terminus and the final alignment was produced in Adobe illustrator.

The Conserved Domain database [20] was searched to identify similarity in domains of the N-terminal region of PhaC. The region upstream the gene encoding BrPhaC (predicted by Prodigal) was further analyzed using the gene predictors GeneMark [21] and Glimmer [22] to identify the correct start codon.

The amino acid composition of the CAP subdomains belonging to BrPhaC, CnPhaC and ChPhaC were analyzed using the PSIPRED server [23]. The GRAVY (grand average of hydropathy) value for the protein sequences was calculated by adding the hydropathy value for each residue and dividing by the length of the sequence [24].

Isolation of the bacterium and identification of the genes

The bacterium from which the *BrphaC* gene was retrieved, *Brevundimonas* sp. KH11J01, was isolated from the Arctic area in Northern Norway, cultured and stored locally at UiT the Arctic University of Norway. The details of sample collection, isolation and 16S RNA identification can be obtained elsewhere [25]. The closest phylogenetic relative according to 16S RNA gene analysis is *Brevundimonas vesicularis* NBRC 12165 (accession number NR_113586.1) with 99% sequence identity. The strain was genome sequenced as part of a larger bioprospecting project at UiT (unpublished data). The contig, containing the *phaC* gene, has been deposited in GenBank under the accession number MW446820. The genes were predicted using Prodigal [26] and annotated using Blast [27]. The gene encoding CnPhaC was retrieved from GenBank using accession code CP039287.1.

Synthesis of target constructs

The two *phaC* genes, encoding BrPhaC and RePhaC, were codon optimized for *Escherichia coli* expression, synthesized and cloned into pET151/D-TOPO expression vector by Invitrogen (Thermo Fisher Scientific, Waltham, MA, USA). The production note from the manufacturer can be obtained in the Supplementary materials section (Suppl. info. 1). Even though the names CnPhaC and RePhaC refer to the same enzyme (PhaC1 enzyme of *C. necator* H16), the former is used when referencing the same PhaC from literature and the latter is used when referring to the enzyme studied here to avoid confusion.

Protein expression and purification

The proteins were expressed in *E. coli BL21*(DE3)* cells (Thermo Fisher Scientific) in 0.5 L Overnight Express™ Instant TB Medium (Novagen) supplemented with 0.4% glycerol. The cells were grown at 37 °C until the optical density (OD) at 600 nm measured by Ultrospec 10 density meter (Cytiva, Marlborough, MA, USA) reached 0.6–0.8 and the cultures were transferred to an incubator-shaker pre-cooled to 15 °C. The cells were left to grow for approximately 20 h and harvested. The pellets were stored at − 20 °C until use.

The pellet was resuspended in 40 ml lysis buffer (20 mM Tris/HCl, 100 mM NaCl) and sonicated for 15 min on ice bath. The lysate was clarified by centrifugation and the crude extract was applied on a HisTrap™ HP 5 ml prepacked Ni-NTA column (Cytiva) equilibrated with lysis buffer plus 10 mM imidazole. The target proteins were eluted using a linear gradient from 10 to 500 mM imidazole. Both target proteins eluted at ~250 mM imidazole. The eluted protein was diluted and purified further using a self-packed 17 ml Source 15 Q column (Cytiva). To remove the 6xHis-tag, the protein solution was incubated with a Tobacco Etch Virus (TEV) protease overnight at 4 °C and applied for the second time on the HisTrap™ column. The final polishing step was performed by size exclusion chromatography (SEC) using HiLoad® Superdex 200 16/60 prep grade prepacked column (Cytiva). The buffers used in the purification process are listed in Supplementary Table 1. AKTA FPLC™ Purifier/Explorer system (GMI, Ramsey, MN, USA) and Unicorn software (Cytiva) were utilized in all steps for execution of the purification and analysis of the results. Unless otherwise specified, all the purification steps were executed at a temperature below 10 °C and the samples were kept on ice.

The fractions containing the target proteins were identified by SDS-polyacrylamide gel electrophoresis (SDS-PAGE) using the Mini-PROTEAN Tetra cell electrophoresis system (Bio-Rad Laboratories, Hercules, CA, USA). The gels were visualized by the Gel doc XR system (Bio-Rad). The concentration of the proteins was measured by a NanoDrop™ 2000/2000c spectrophotometer (Thermo Fisher Scientific).

Molecular weight determination by SEC

The pure protein samples (5 mg/ml, 0.5 ml) were loaded onto a prepacked HiLoad® superdex 200 16/60 prep grade column (Cytiva) equilibrated with a buffer containing 50 mM Tris/HCl (pH 8.0) and 150 mM NaCl. PhaCs were eluted with the same buffer at a flow rate of 1 ml/min, and the fractions corresponding to the peaks were assayed for PhaC activity and by SDS-PAGE. Molecular weights were determined from a calibration curve prepared using the following protein molecular weight standards (Suppl. Fig. 4): ferritin (440 kDa), aldolase (158 kDa), covalbumin (75 kDa), ovalbumin (44 kDa), carbonic anhydrase (29 kDa), and ribonuclease A (13.7 kDa).

PhaC activity measurement

The Ellman's methods for assaying PhaC activity were adapted from [28] with some modifications. Two different approaches were used.

The discontinuous enzyme assay: The standard reaction was carried

out at 30 °C in a reaction volume of 200 µL consisting of 100 mM potassium phosphate (pH 7.4), 2 mM 3-hydroxybutyryl-CoA (3HBCoA), 0.2 mg/ml (3 µM) bovine serum albumin (BSA) and PhaC. Aliquots of 20 µL were removed at different time intervals, incubated on ice for 2 min before mixing with 20 µL ice cold 10% (w/v) trichloroacetic acid to quench the reaction. After centrifuging the reaction mixture, 35 µL was added to 125 µL of a freshly prepared solution of 2 mM 5,5-dithio-bis-(2-nitrobenzoic acid) (DTNB) in 100 mM phosphate (pH 7.4) in a clear 96-well microtiter plate. Using a microplate reader (SpectraMax M4, Molecular Devices, San Jose, CA, USA), the end point absorbance at 412 nm ($\varepsilon = 14.15\ mM^{-1}\ cm^{-1}$) was measured after incubation for 5 min at room temperature. All the reaction components except the substrate were included in the blank runs, and the blank read was subtracted from all sample reads.

The continuous enzyme assay: This assay was preferred when assaying pure enzymes. The reactions were carried out in a clear 96- well microtiter plate at 25 °C in a final volume of 100 µL consisting of 100 mM potassium phosphate pH 7.4, 0.3 mM DTNB, 0.2 mg/ml BSA, 2 mM 3HBCoA, and the synthase at different concentrations. The reaction was initiated by addition of the purified enzyme. Formation of TNB dianion was determined by measuring absorbance at 412 nm using an extinct coefficient of 14.15 $mM^{-1}\ cm^{-1}$ in a microtiter plate reader (SpectraMaxM4, Molecular Devices). All the reaction components except the enzyme were included in the blank runs, and the blank read was automatically subtracted from all sample reads. The reaction rate was determined from the slope of the initial fast phase. One unit is defined as 1 µmol of substrate consumed per min.

Determination of temperature, salt and pH optima for enzyme activity

For these experiments, the enzyme activities were measured using the discontinuous assay. Appropriate reaction time (2 min for BrPhaC and 4 min for RePhaC) was set after evaluating the linearity of the activity of each enzyme and the intensity of the absorbance signal at the respective time points. Salt and pH optima for the activity of BrPhaC and RePhaC were determined at 35 °C and 30 °C, respectively. The samples were run in 3 parallels. The same protein concentration was used for each enzyme throughout the experiments. The activity was calculated relative to the maximum activity measured from the whole range.

The activities of BrPhaC and RePhaC were measured at 5 °C intervals ranging from 10 to 55 °C to determine their temperature optima. Crude cell extracts were freshly prepared by sonication and clarification. As shown in Supplementary Fig. 1, the expression level of the soluble fraction of both enzymes was similar. A reaction mixture of 20 µL volume was incubated for 2/4 min at each temperature and endpoint measurement was performed. The activity of BrPhaC and RePhaC were measured in the standard discontinuous assay at 15, 30 and 45 °C to study the shape of the activity curve and the nature of the lag-phase.

To determine the NaCl concentration and pH optima, the activities of BrPhaC and RePhaC were measured in different NaCl concentrations (0–400 mM) and pH (6.0–9.0). Three different buffers were used in their useful pH ranges: Bis-Tris propane (6.3–9.5), HEPES (6.8–8.2) and Tris/HCl (7.0–9.0) for determination of the pH optimum. A reaction mixture of 20 µL volume containing 1.3 and 1.6 µM purified BrPhaC and RePhaC, respectively, was used in these experiments.

Differential scanning calorimetry (DSC)

DSC experiments were conducted using a Nano-Differential Scanning Calorimeter III, model CSC6300 (Calorimetry Sciences Corporation, Lindon, UT, USA). The enzymes were dialyzed overnight at 4 °C against 1 L of dialysis buffer (50 mM HEPES pH 7.4, 100 mM NaCl) in a Pierce SlideA-Lyzer dialysis cassettes (Thermo Fisher Scientific) with a 30 kDa cut-off followed by filtration using a 0.2 µm syringe filter (Merck). The dialysis buffers were used as reference buffers in the DSC runs. Reference buffers and samples were degassed under vacuum for 10 min before loading into the respective DSC cells. The temperature scans were carried out at a constant pressure of 0.3 MPa in a range of 25–80 °C with a heating/cooling rate of 1 °C/min. NanoAnalyzer software (TA instruments, New Castle, DE, USA) was utilized to determine the melting temperature and molar heat capacity values. The experimental transition curves were fitted on a two-state transition model.

Determination of kinetic parameters

Kinetic experiments were performed by the continuous assay for BrPhaC at 25 °C as described above. The assays were conducted at concentrations of 3HBCoA varying from 0.1 to 4 mM and 3 nM enzyme. The measurements were performed in triplicate for each substrate concentration. The initial velocity of the enzyme at each substrate concentration was calculated from the slope of the first linear phase and the kinetic parameters k_{cat} and K_m were determined by fitting the data to the Michaelis–Menten equation using the EnzymeKinetics® module in SigmaPlot 14 (SYSSTAT).

Result and discussion

Identifying the correct start of the BrphaC gene

Identifying the correct start of the *phaC* gene in *Brevundimonas* sp. KH11J01 was not straightforward. Homologs within the same genus are annotated to start at MAKT- or LIET- (Suppl. Fig. 2). Prodigal predicts a longer gene than GeneMark and Glimmer. A manual analysis was performed of the short version of all the *Brevundimonas phaC* genes found in Genbank and conserved regions upstream of the erroneous prematurely predicted start-codon were observed. In addition, a short version of the closely related *Caulobacter crescentus* PhaC (CcPhaC) has been expressed and found less active, whereas the long version is fully active [29]. A publication analyzing the Ribosomal Binding Site (Shine-Dalgarno sequence) *in C. crecentus,* a close relative of *Brevundimonas*, revealed that this bacterium uses a classical ribosome binding site in front of only 24.6% of its genes. The reannotated genome of *C. crecentus* NA1000 [30] predicts a much longer *phaC* gene based on transcriptomic data. In order not to clone too short a BrPhaC construct, it was decided to use the length of the *C. crecentus phaC* gene as a guide when cloning the *Brevundimonas phaC* gene. After manual inspection of the region upstream of the potential start methionines (Suppl. Fig. 2) the longest one was cloned, starting with MNRP-.

The search against the conserved domain database (CDD) gave a hit against the PhaC protein but also towards the τ subunit of bacterial DNA polymerase III (cdd accession: PRK07764) (Suppl. Fig. 3).

Pure and active BrPhaC and RePhaC were produced in large amounts

BrPhaC and RePhaC were overexpressed in *E. coli BL21*(DE3)* cells and purified to more than 95% apparent purity as judged by SDS-PAGE (Fig. 1). The purification strategy is summarized in Table 1 and Table 2. The protein yields at the end of the purification were 4.9% for BrPhaC and 15.5% for RePhaC corresponding to a total protein amount of 41.4 mg and 120 mg, respectively. The specific activities of both enzymes measured after the last purification step were similar, 59.8 and 61.9 U/mg for BrPhaC and RePhaC, respectively.

The purification strategy developed for BrPhaC was applied to RePhaC and resulted in 240 mg pure and active enzyme per liter bacterial culture. Hence, this purification strategy offers the possibility of studying PhaCs by methods which require large amounts of pure protein. The number of steps was higher in this study than in earlier reports [31,32] to remove the DNA contaminants in the sample and the affinity tag. The enzyme was pure after the first step (Fig. 1B). Thus, it is possible to omit some of the steps and go directly to the last step unless one is concerned to remove the affinity tag and DNA contaminants in the sample. Different specific activity values ranging from 1 to 160 U/mg

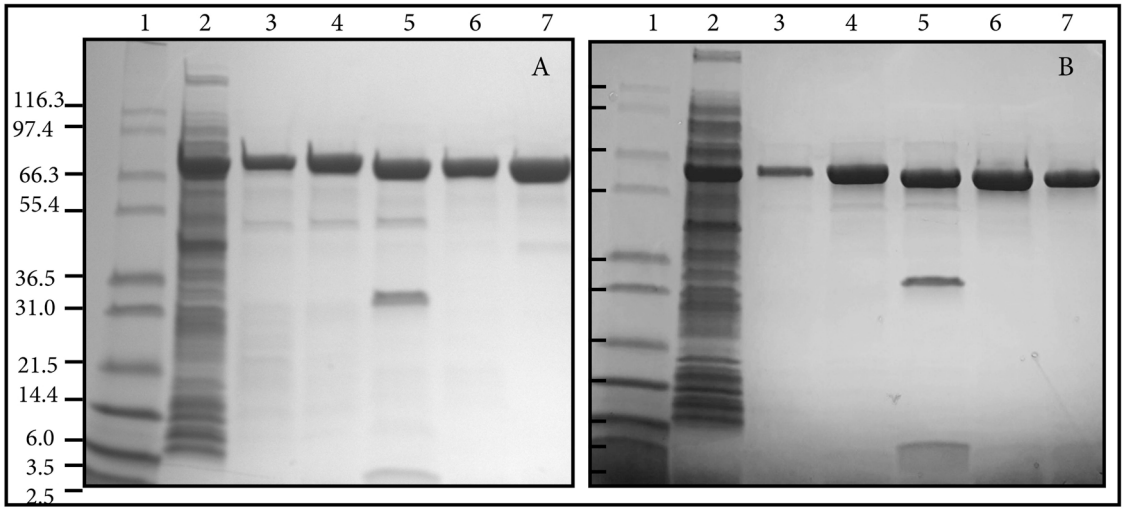

Fig. 1. Purification of BrPhaC (A) and RePhaC (B): SDS-PAGE gel showing the protein contents of the fractions after each step. Lane 1, Mark12™ protein molecular weight marker; Lane 2, Crude cell extract; Lane 3, HisTrap 1 fraction; Lane 4, Source 15Q fraction; Lane 5, the fraction after TEV cleavage reaction; Lane 6, HisTrap 2 fraction; Lane 7, SEC fraction.

Table 1
A purification summary table for BrPhaC.

Fractions	Volume (ml)	Enzyme Activity (U/ml)	Protein Concentration (mg/ml)	Total Protein (mg)	Total Activity (U)	Specific Actvity (U/mg)	Yield (%)	Purification fold
Crude extract	45	1121.0 ± 12.1	175.0 ± 1.5	7875.0	50,445.8	6.4	100	1
HisTrap 1	145	56.8 ± 0.5	1.8 ± 0.2	256.4	8240.3	32.1	16.3	5.0
Source 15Q	37	196.0 ± 6.6	2.7 ± 0.4	99.2	7250.4	73.1	14.4	11.4
After TEV cleavage	40	275.1 ± 3.9	2.7 ± 0.7	106.2	11,005.3	103.6	21.8	16.2
HisTrap 2	62	44.1 ± 0.8	0.9 ± 0.1	53.3	2736.2	51.4	5.4	8.0
SEC	35	70.8 ± 1.2	1.2 ± 0.1	**41.4**	2476.5	**59.8**	4.9	9.3

Table 2
A purification summary table for RePhaC.

Fractions	Volume (ml)	Enzyme Activity (U/ml)	Protein Concentration (mg/ml)	Total Protein (mg)	Total Activity (U)	Specific Actvity (U/mg)	Yield (%)	Purification fold
Crude extract	42	1138.5 ± 10.9	136.9 ± 2.1	5749.3	47,815.0	8.3	100	1
HisTrap 1	45	353.9 ± 5.4	5.3 ± 0.6	236.7	15,926.1	67.3	33.3	8.1
Source 15Q	30	999.0 ± 2.6	5.9 ± 0.3	177.8	29,969.4	168.5	62.7	20.3
After TEV cleavage	48	198.7 ± 3.4	4.0 ± 0.3	190.0	9540.0	50.2	20.0	6.0
HisTrap 2	55	167.8 ± 3.2	3.1 ± 0.4	173.0	9217.2	53.3	19.3	6.4
SEC	50	148.7 ± 1.6	2.4 ± 0.1	**120.0**	7433.5	**61.9**	15.5	7.5

have been reported for purified CnPhaC [31], and RePhaC falls in this range with 61.9 U/mg specific activity. Such a variation was believed to arise because of inconsistent use of reaction components and utilization of different methods for protein expression, concentration determination, and purification.

Enzyme properties of BrPhaC and RePhaC

BrPhaC shows a broader temperature-activity profile

The temperature at which the maximum activity was measured (T_{max}) was 35 °C for BrPhaC and 30 °C for RePhaC. BrPhaC showed higher activity over a broader temperature range, while the range was narrower and towards higher temperature for RePhaC (Fig. 2A). The effect of NaCl concentration on the enzyme activity was very similar for both enzymes (Fig. 2B). The maximal activity was measured for both at NaCl concentrations ranging from 0 to 50 mM, with the activity of both enzymes dropping dramatically above this concentration. The pH at maximum activity was 8.5 for BrPhaC and 7.5 for RePhaC. BrPhaC maintain at least 75% of maximal activity in the pH range from 7.0 to 9.0 (Fig. 2C), while RePhaC gave at least 60% of the maximal activity in the pH range 7.0–8.5 (Fig. 2D).

BrPhaC does not require priming or activation to initiate the polymerization reaction

A lag-phase of several seconds has been observed for CnPhaC and many other PhaCs [29,31,33]. The delay is believed to occur as a result

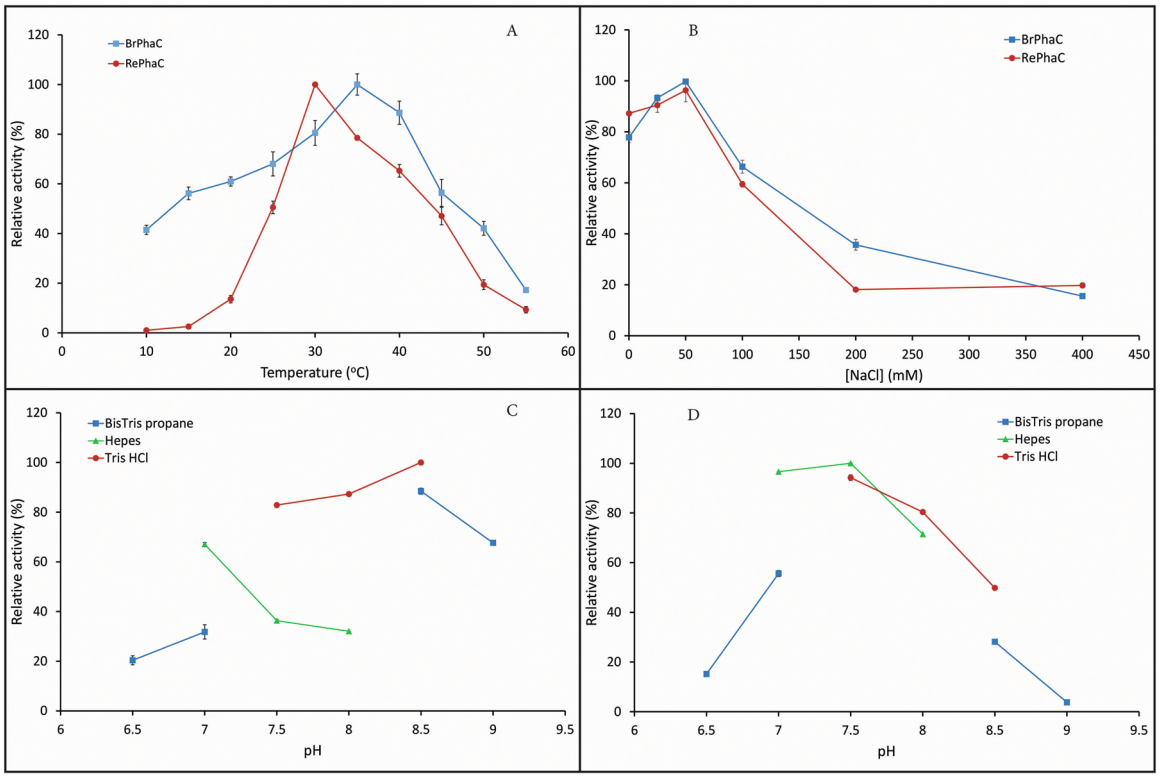

Fig. 2. Basic enzymatic characterization of BrPhaC and RePhaC. A; temperature optimum for activity of BrPhaC (Blue line with square points) and RePhaC (Red line with solid circles). B; NaCl concentration optimum for activity of BrPhaC (Blue line with square points) and RePhaC (Red line with solid circles). pH optimum for the activity of BrPhaC (C) and RePhaC (D), Blue line with square points represents BisTris Propane buffer, green line with triangles represents HEPES buffer and red line with solid circles represents Tis/HCl buffer. The error bars indicate the standard deviation of the results from duplicate/triplicate measurements.

of the time required for priming and protein dimerization, necessary for the initiation of the enzymatic reaction [29]. Priming with a protein interaction partner such as PhaM, detergents, trimeric HBCoA analogs and multihydroxyl compounds like fructose are among the methods reported to shorten or eliminate the lag-phase [28,29,33,34]. PhaM from *C. necator* H16 is a granule-associated protein that serves as a natural primer or activator of PhaC activity by facilitating oligomerization of PhaC and shortening the lag-phase as a result [34]. The nature of the activity shape of BrPhaC was studied and compared to RePhaC at three different temperatures. As shown in Fig. 3, the lag-phase was absent, and the shape of the curves was unaffected by the temperature change for BrPhaC, unlike for RePhaC where the initiation of the reaction was highly dependent on temperature change. This observation may indicate that the BrPhaC has already adopted the necessary conformational changes before binding to the substrate. To the best of our knowledge, BrPhaC is one of the three PhaCs, which are reported not to exhibit a lag-phase. Class I PhaCs from *C. crescentus* (CcPhaC) [29] and from the purple photosynthetic bacterium *Rhodovulum sulfidophilum* (RsPhaC) [35] are the other two PhaCs which lack a lag-phase. Interestingly, all of these belong to the Alphaproteobacteria.

Kinetic properties of BrPhaC

The Michaelis-Menten fitting of the data is shown in Fig. 4. V_{max}, K_m and k_{cat} values are 10.3 µmol/min/mg, 0.63 mM and 12.0 s^{-1} respectively. It was observed that storing the enzyme at even − 80 °C reduced the activity. Therefore, caution should be taken when interpreting the k_{cat} by taking into consideration that this can underestimate the specific activity of the enzyme, the V_{max} and then the k_{cat}. K_m is apparently not affected by this. Because of the presence of a lag-phase, the enzyme kinetics of the RePhaC were not determined in this study.

Two studies have reported kinetic parameters of PhaC. One was performed on a lag-phase free CnPhaC achieved by adding 70% fructose to the reaction mixture [33]. The authors argued that the multihydroxyl compound fructose activates the enzyme to undergo dimerization and eliminates the lag-phase. The K_m, which is a reflection of the affinity of the enzyme towards the substrate, documented for 3HBCoA as substrate was five times lower than that observed for BrPhaC in this study. Considering the experimental condition used in that study, which was far from the physiological conditions of the enzyme, it is difficult to compare the results as they are. In the other study, the K_m determined for CcPhaC using 3HBCoA as substrate was almost half that reported for BrPhaC here [29]. The attempt to determine the kinetic parameters of another naturally lag-phase free class I PhaC, RsPhaC, failed because the activity never reached a plateau even at a very high substrate concentration [35].

The oligomeric state of the PhaCs

The functional BrPhaC exists uniquely as a trimer

PhaCs of all enzyme classes exist as either homo- or hetero- oligomers and oligomer formation is important for their polymerization activity [33,36]. Most PhaCs have been found to exist in an equilibrium between the monomeric and dimeric forms *in vitro* [14,15,32,33,37], and the presence of the substrate is believed to induce the dimerization [14,15]. BrPhaC eluted in a single peak only (Fig. 5A), corresponding to a homotrimer as verified by SDS-PAGE (Lane 5, Fig. 5B) and PhaC activity measurement (data not shown). The molecular weight estimated according to the calibration curve of the column was 226 kDa, which is approximately three times the size of the monomeric protein (Table 3, Suppl. Fig. 4). This appears to be the first report of a trimeric PhaC. Others have similarly reported that RsPhaC exists only as a functional dimer in the absence of a substrate [35]. The addition of 3HB-CoA in

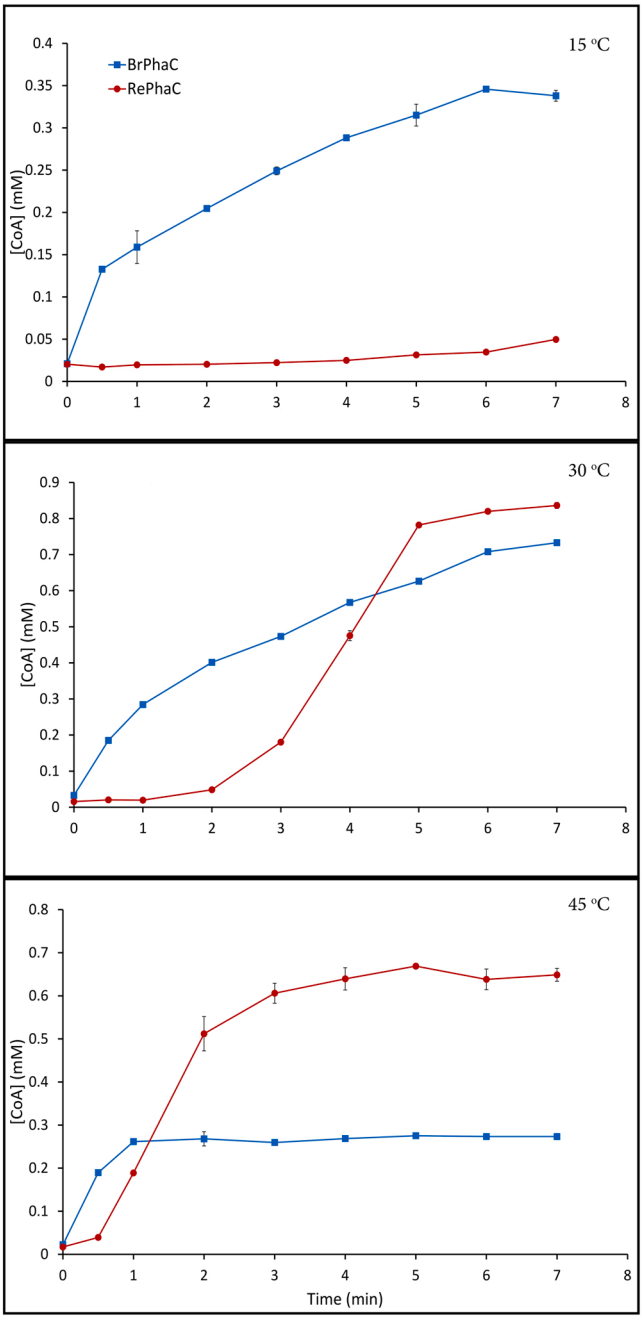

Fig. 3. The time-wise activity pattern of BrPhaC (Blue line with square points) and RePhaC (Red line with solid circles) at 15 °C, 30 °C and 45 °C in a discontinuous assay. The error bars indicate the standard deviation of the results from triplicate measurements.

different concentrations barely affected the dimerization profile. In another study that focused on the chain termination mechanisms of CcPhaC (which originates from the same bacterial family as the *Brevundimonas* genus), a migration of CcPhaC between dimeric or trimeric forms was observed [29]. As for BrPhaC, the reactions of RsPhaC and CcPhaC start instantly without a lag-phase.

The charge profile of the CAP subdomain of BrPhaC does not support a dimeric structure

The sequence of the CAP subdomain region in BrPhaC (422–541) is more polar than the homologous CAP subdomain of CnPhaC (347–471) and ChPhaC (319–471) (Suppl. Fig. 5). Larger hydrophobic residues are

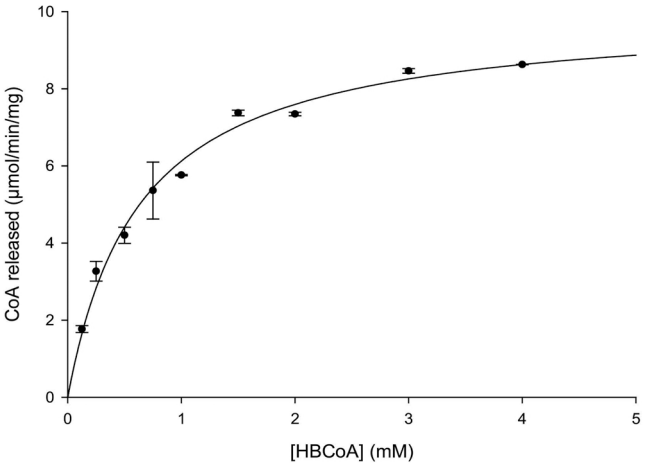

Fig. 4. Michaelis-Menton enzyme kinetics of BrPhaC: the specific activity of the enzyme is plotted against the substrate concentration. V_{max} = 10.3 µmol min^{-1} mg^{-1}, K_m = 0.63 mM, k_{cat} = 12.0 S^{-1}, k_{cat}/K_m = 19.0 S^{-1} mM^{-1} The error bars indicate the standard deviation of the results from triplicate measurements.

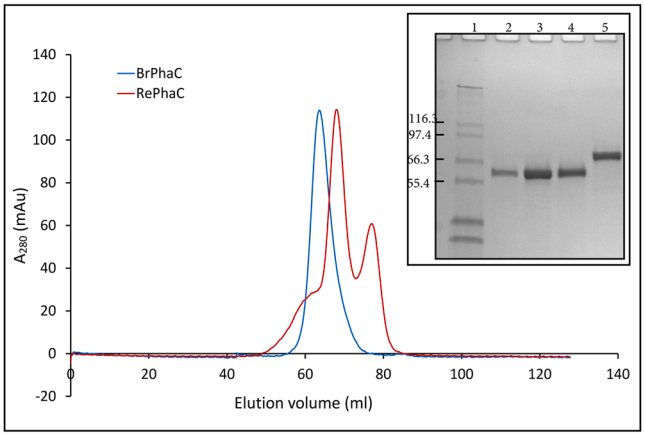

Fig. 5. Molecular weight determination of BrPhaC and RePhaC by size-exclusion chromatography. The chromatograph for elution of BrPhaC (blue line) and RePhaC (red line) and SDS-PAGE gel after SEC molecular size analysis are shown. Lane 1, Mark12™ protein standard marker; Lane 2, RePhaC peak 1; Lane 3, RePhaC peak 2; Lane 4, RePhaC peak 3; Lane 5, BrPhaC.

replaced by smaller and less hydrophobic ones, and the number of polar /charged amino acids is higher (Negative GRAVY scale for BrPhaC). This observation implies that the domain is likely to be a more solvent exposed area rather than that facing the other protomer. This finding may indicate that BrPhaC monomers can have other intermolecular contact points resulting in a different oligomerization characteristic. Despite several trials, efforts to determine the crystal structure of BrPhaC only resulted in poorly diffracting crystals (Suppl. Info. 2 and Suppl. Fig. 6). It was therefore not possible to study the intermolecular contacts and forces. It is considered unlikely that the trimeric structure of BrPhaC is stabilized by intermolecular disulfide bridges in the non-reducing buffer environment as mentioned elsewhere for other PhaCs [13–15]. There are only two cysteines in the sequence of BrPhaC including the catalytic Cys394, while CnPhaC has five. It is therefore impossible for the other cysteine to take part in a trimeric organization of BrPhaC protomers.

Dimer formation in RePhaC is not necessarily mediated by substrate binding

RePhaC was eluted in three different peaks (Fig. 5A) corresponding

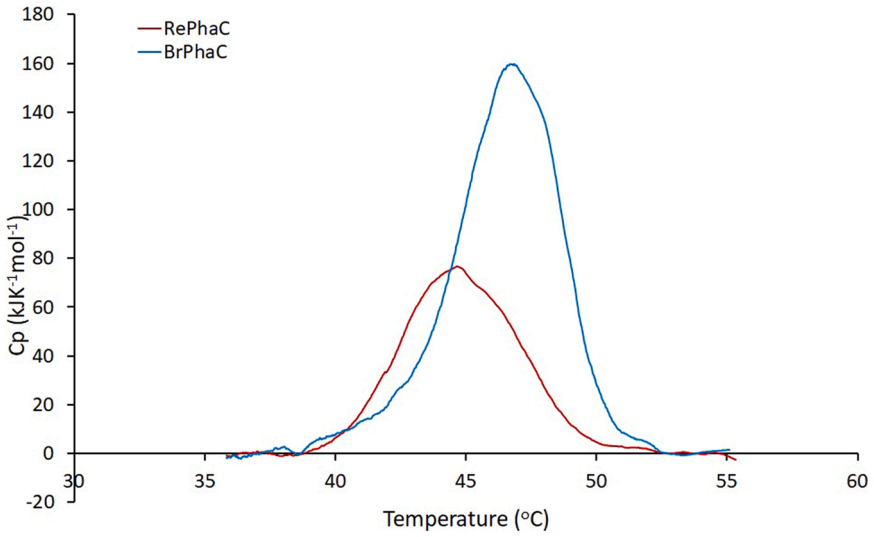

Fig. 6. A melting curve of BrPhaC (blue line) and RePhaC (red line) after DSC. Melting temperature (T_m) and ΔH respectively: BrPhaC, 47.1 °C and 692.9 kJ mol^{-1}; RePhaC, 44.5 °C and 482.8 kJ mol^{-1}.

Table 3
Determination of molecular weights of BrPhaC and RePhaC by size exclusion chromatography.

Protein	Theoretical monomeric MW (kDa)	Experimental MW (kDa)
BrPhaC	71.9	226.4 ± 5.1
RePhaC	64.2	
Peak 1		250.5 ± 31.7
Peak 2		132.6 ± 19.5
Peak 3		67.3 ± 5.1

to a tetramer, dimer and monomer, and the respective sizes of the peaks were 250.5, 132.6 and 67.3 kDa (Table 3), in agreement with what was reported previously [14,15,32,33]. All three peaks correspond to RePhaC as verified by SDS-PAGE (Lane 2, 3 and 4 in Fig. 5B). PhaC activity was detected only in the dimeric form (data not shown). In spite of the absence of a substrate, the dimeric form of RePhaC was clearly the dominant one in this study, unlike what was reported elsewhere [14,32,33]. This indicates that dimer formation is not solely regulated by substrate binding and other factors might also play an important role. The dimer is the active form of the enzyme [28].

The unstructured and positively charged N-terminal domain of BrPhaC could be implicated in oligomerization and DNA binding

Despite the availability of the crystal structures of the catalytic domain of two PhaCs, the understanding of the mechanism of dimer formation and catalysis remains limited, as the structures presented represent a non-active form. The catalytic domain of PhaC exhibits only a trace amount of activity without the N-terminal domain both *in vivo* and *in vitro* [14,38]. It has been shown that the N-terminal domain is implicated in the PhaC activity, substrate specificity, dimer formation and determination of the molecular weight of PHA polymers [16,37,38].

The N-terminal domain of BrPhaC is unique as it has an extra unstructured region at the start of the protein (aa 1–72) (Fig. 7). This extra extension was found only in PhaC sequences belonging to the *Caulobacterales* family. Using the BrPhaC in a search against the conserved domain database (CDD) [20] gave a hit in the N-terminus (aa 10–191) towards the τ subunit of bacterial DNA polymerase III (cdd accession: PRK07764) (Suppl. Fig. 3), more specifically towards a proline-rich tether and the start of domain IV. This region is thought to be a putative DNA interaction site [39]. Thus, we speculate that this region ties the PhaC protein and possibly also the growing PHA granule to the bacterial DNA. The positive charge of the unstructured domain also fits with this hypothesis. An analysis of all *Caulobacterales* PhaC sequences reveals that the positively charged region is present and contains many prolines, alanines, arginines and lysines (data not shown). The region is unstructured, has variable length and has no apparent sequence conservation. Interestingly a mutant CcPhaC with the first 85 amino acids removed, has been characterized [29]. When measuring activity, this enzyme had a lag-phase while the full-length protein did not. This suggests that the N-terminal disordered positively charged peptide might also strengthen/stabilize the oligomeric state of the functional PhaC, either by protein-protein interaction or protein-DNA interaction. Another interesting similarity is towards the PhaM protein found in *C. necator*. This protein is shown to associate with PhaC, stabilize the dimer, remove the lag-phase and bind DNA [34]. The DNA binding region of PhaM has been investigated and a 2X PAKKA motif, located in the C-terminal, is found to be important for the DNA binding. This unstructured, C-terminal DNA-binding region of PhaM resembles that of the unstructured N-terminal region of BrPhaC. The role of BrPhaC's exceptionally long N-terminal domain (1–276) in the oligomeric organization of the enzyme remains to be investigated. Such unstructured and positively charged C-terminal extension was also observed in PhaCs from *Cobetia* [40].

Thermal adaptation of BrPhaC

BrPhaC shows cold-adapted features

The BrPhaC has cold-active features as it retains much of its activity when reducing the temperature below 20 °C. RePhaC is nearly inactive at 10 °C, whereas BrPhaC is still 40% active (Fig. 2A). Such cold-adapted activity or cold activity is one of the distinctive features of enzymes from organisms inhabiting a cold environment [41]. The cold activity of BrPhaC is not a surprising finding because it originates from a bacterium isolated from the Barents Sea. In addition, the higher K_m value reported for BrPhaC reveals its lower affinity towards 3HBCoA substrate. Such a tendency of reduced affinity towards their substrate is one of the features of cold-adapted enzymes [42]. The reduced substrate binding affinity is believed to compensate for the detrimental effect of low temperature. The results from this study indicate that BrPhaC indeed shows thermal adaptation features, and temperature affects the

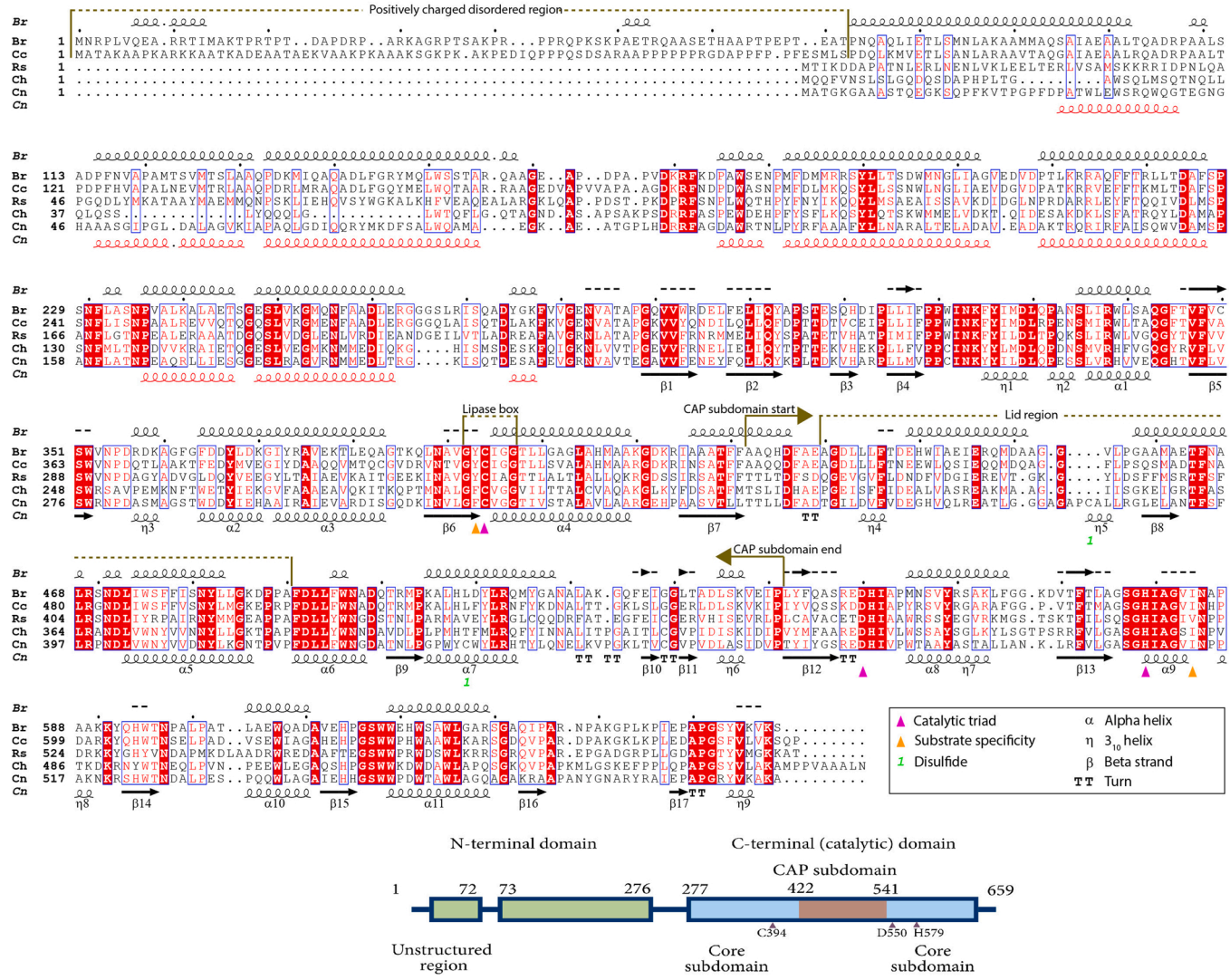

Fig. 7. Sequence alignment of selected type I PhaCs. The origin of the sequences and their accession numbers are: Br (*Brevundimonas* sp. KH11J01, acc nr. MW446820), Cc (*Caulobacter crescentus* NA1000, acc nr. YP_002516817.4), Rs (*Rhodovulum sulfidophilum* DSM 1374, acc nr. ANB35720.1), Ch (*Chromobacterium* sp. USM2, acc nr. ADL70203.1) and Cn (*Cupriavidus necator* H16, acc nr. CAJ92572). The predicted secondary structure belonging to BrPhaC is shown above the alignment. The predicted secondary structure of the N-terminal domain belonging to CnPhaC, together with the secondary structure extracted from the catalytical domain x-ray structure (PDB id 5T6O) is shown below the alignment in red and black, respectively. The location of the CAP subdomain and Lid region is also indicated. The domain organization of BrPhaC is shown. BrPhaC consists of two domains, the N-terminal domain (1–276 in green) the C-terminal (catalytic) domain (277–659) containing the catalytic triad residues C394, D550 and H579 (shown as triangle marks). The catalytic domain consists of the core subdomain (277–421, 542–659, pale blue) and the CAP subdomain (422–541, light brown). The N-terminal domain comprises the unstructured region (1–72).

initiation of polymerization and the catalytic activity to a lesser extent than for RePhaC. This is in line with the theory that cold-adapted enzymes tend to reduce the dependence on temperature [41].

The higher thermal stability of BrPhaC than RePhaC could arise from a need for local flexibility without losing its overall compact structure

The absence of other oligomeric forms apart from the trimer can be explained by a compact structure of the trimeric BrPhaC [35]. The DSC analysis indeed showed a higher melting temperature (T_m) for BrPhaC (47.1 °C) than RePhaC (44.5 °C) (Fig. 6). This is the first study to report the T_m of the PhaC from *C. necator* H16 as measured by DSC analysis. The thermal liability of the enzyme was briefly studied earlier by using heat inactivation assay [43]. Both the melting temperature difference of 2.6 °C and a very large difference in the enthalpy of unfolding (Suppl. Table 2) are characteristics of a more compact structure of BrPhaC [44]. Being a cold active enzyme, one would expect that the T_m for BrPhaC was lower than that for RePhaC. However, the trimeric organization of the BrPhaC enzyme may lead to an overall more stable structure, despite being cold-adapted. It can be hypothesized that the trimeric organization seen for BrPhaC is more stable than the dimeric organization seen for RePhaC. This could be due to a higher degree of subunit interactions, as seen for other proteins [45].

Enzymes from microorganisms adapted to low temperatures tend to show thermal adaptation features such as increased specific activity at low temperatures at the expense of reduced stability [42,44]. That is not the case for this PhaC from the bacterium isolated from the Arctic environment. Considering the cold activity of BrPhaC mentioned above, it is reasonable to assume that the enzyme may display a local flexibility without losing its compact structure as a whole. Cold-adapted enzymes are typically characterized by an improved flexibility of the structural regions involved in catalysis, whereas other protein regions not implicated in catalysis may be even more rigid than their mesophilic counterparts [41,42].

The implication of cold-adapted PhaC to an energy-efficient PHA production

The results from this study reveal the cold-adapted features of BrPhaC. This may not have a direct relevance for PHA production, as *in vitro* synthesis of PHA using PhaC enzymes and PHA monomers by itself is expensive. Investigation of the microbial PHA synthesis machinery at a molecular level would rather increase understanding of the polymer formation that can be inferred to the organism level. The bacterium from which BrPhaC originated from, *Brevundimonas* sp. KH11J01, grows and produces PHA optimally indeed at ambient temperature (25 °C) in a medium of mild salinity (unpublished data). This is in agreement with the *in vitro* results reported here. The efforts to reduce the cost of PHA production focus mainly on utilization of low-cost carbon sources as feedstocks for the bacteria [46–48]. Energy efficient PHA production can be another area of cost reduction. The cost related to heating or cooling can be spared by using cold-adapted microorganisms harboring cold-active enzymes for PHA production at ambient temperatures. Exploiting the unique features of extremophiles for the economic benefits of PHA production has been recently discussed [49]. The trimeric BrPhaC with an increased stability and activity could also be beneficial in normal industrial settings.

Concluding remarks

The currently accepted catalytic mechanism of type I PhaC assumes that the dimer is the active form of the enzyme. The report of a functional PhaC with its trimeric organization in this study further complicates our understanding. It is possible that the available crystal structures, of the catalytical domain alone, do not properly reveal how the complete enzyme is assembled. A full-length crystal structure of BrPhaC is being pursued, although the high degree of flexibility within and between the domains makes this very challenging. The involvement of the PHA granules, other protein partners (PhaM in the case of CnPhaC) and possibly also DNA must be dissected to fully understand this enzyme class. It is clear that further structural and mutational studies are required to have a better understanding of the oligomerization and catalytic mechanisms of BrPhaC in full detail.

Funding

The project was financed by the Research Council of Norway (Grant no.: 270308).

CRediT authorship contribution statement

NGA designed and conducted the laboratory experiments, analyzed the data, drafted the manuscript, and compiled the final version. BA performed and presented the theoretical work. BA and HH supervised the work. All contributed in developing the drafted manuscript, read and approved the final version.

Declaration of Competing Interest

The authors declare no conflicts of interest.

Appendix A. Supporting information

Supplementary data associated with this article can be found in the online version at doi:10.1016/j.nbt.2022.05.003.

References

[1] Chen YJ, Tsai PC, Hsu CH, Lee CY. Critical residues of class II PHA synthase for expanding the substrate specificity and enhancing the biosynthesis of polyhydroxyalkanoate. Enzyme Microb Technol 2014;56:60–6. https://doi.org/10.1016/j.enzmictec.2014.01.005.

[2] Anderson AJ, Dawes EA. Occurrence, metabolism, metabolic role, and industrial uses of bacterial polyhydroxyalkanoates. Microbiol Rev 1990;54(4):450–72. https://doi.org/10.1128/mr.54.4.450-472.1990.

[3] Obruca S, Sedlacek P, Koller M. The underexplored role of diverse stress factors in microbial biopolymer synthesis. Bioresour Technol 2021;326:124767. https://doi.org/10.1016/j.biortech.2021.124767.

[4] Obruca S, Sedlacek P, Slaninova E, Fritz I, Daffert C, Meixner K, et al. Novel unexpected functions of PHA granules. Appl Microbiol Biotechnol 2020;104(11):4795–810. https://doi.org/10.1007/s00253-020-10568-1.

[5] Anjum A, Zuber M, Zia KM, Noreen A, Anjum MN, Tabasum S. Microbial production of polyhydroxyalkanoates (PHAs) and its copolymers: a review of recent advancements. Int J Biol Macromol 2016;89:161–74. https://doi.org/10.1016/j.ijbiomac.2016.04.069.

[6] Park SJ, Hong SH, Lee SY. Polymerisation of building blocks to macromolecules: polyhydroxyalkanoates as an example. In: Smolke CD, editor. The metabolic pathway engineering handbook. Boca Raton, FL, USA: CRC Press; 2010. p. 1–19.

[7] Sheu DS, Lee CY. Altering the substrate specificity of polyhydroxyalkanoate synthase 1 derived from *Pseudomonas putida* GPo1 by localized semirandom mutagenesis. J Bacteriol 2004;186:4177–84. https://doi.org/10.1128/JB.186.13.4177-4184.2004.

[8] Park SJ, Kim TW, Kim MK, Lee SY, Lim SC. Advanced bacterial polyhydroxyalkanoates: towards a versatile and sustainable platform for unnatural tailor-made polyesters. Biotechnol Adv 2012;30(6):1196–206. https://doi.org/10.1016/j.biotechadv.2011.11.007.

[9] Potter M, Steinbuchel A. Poly(3-hydroxybutyrate) granule-associated proteins: impacts on poly(3-hydroxybutyrate) synthesis and degradation. Biomacromolecules 2005;6(2):552–60. https://doi.org/10.1021/bm049401n.

[10] Tan IKP, Foong CP, Tan HT, Lim H, Zain NA, Tan YC, et al. Polyhydroxyalkanoate (PHA) synthase genes and PHA-associated gene clusters in *Pseudomonas* spp. and *Janthinobacterium* spp. isolated from Antarctica. J Biotechnol 2020;313:18–28. https://doi.org/10.1016/j.jbiotec.2020.03.006.

[11] Chen GQ, Patel MK. Plastics derived from biological sources: present and future: a technical and environmental review. Chem Rev 2012;112(4):2082–99. https://doi.org/10.1021/cr200162d.

[12] Chek MF, Hiroe A, Hakoshima T, Sudesh K, Taguchi S. PHA synthase (PhaC): interpreting the functions of bioplastic-producing enzyme from a structural perspective. Appl Microbiol Biotechnol 2019;103(3):1131–41. https://doi.org/10.1007/s00253-018-9538-8.

[13] Wittenborn EC, Jost M, Wei Y, Stubbe J, Drennan CL. Structure of the catalytic domain of the class I polyhydroxybutyrate synthase from *Cupriavidus necator*. J Biol Chem 2016;291(48):25264–77. https://doi.org/10.1074/jbc.M116.756833.

[14] Kim J, Kim YJ, Choi SY, Lee SY, Kim KJ. Crystal structure of *Ralstonia eutropha* polyhydroxyalkanoate synthase C-terminal domain and reaction mechanisms. Biotechnol J 2017;12(1). https://doi.org/10.1002/biot.201600648.

[15] Chek MF, Kim SY, Mori T, Arsad H, Samian MR, Sudesh K, et al. Structure of polyhydroxyalkanoate (PHA) synthase PhaC from *Chromobacterium* sp. USM2, producing biodegradable plastics. Sci Rep 2017;7(1):5312. https://doi.org/10.1038/s41598-017-05509-4.

[16] Chek MF, Kim SY, Mori T, Tan HT, Sudesh K, Hakoshima T. Asymmetric open-closed dimer mechanism of polyhydroxyalkanoate synthase PhaC. iScience 2020;23(5):101084. https://doi.org/10.1016/j.isci.2020.101084.

[17] Notredame C, Higgins DG, Heringa J. T-Coffee: a novel method for fast and accurate multiple sequence alignment. J Mol Biol 2000;302(1):205–17. https://doi.org/10.1006/jmbi.2000.4042.

[18] Robert X, Gouet P. Deciphering key features in protein structures with the new ENDscript server. Nucleic Acids Res 2014;42:W320–4. https://doi.org/10.1093/nar/gku316.

[19] Jones DT. Protein secondary structure prediction based on position-specific scoring matrices. J Mol Biol 1999;292(2):195–202. https://doi.org/10.1006/jmbi.1999.3091.

[20] Lu S, Wang J, Chitsaz F, Derbyshire MK, Geer RC, Gonzales NR, et al. CDD/SPARCLE: the conserved domain database in 2020. Nucleic Acids Res 2020;48(D1):D265–8. https://doi.org/10.1093/nar/gkz991.

[21] Borodovsky M, McIninch J. GeneMark: parallel gene recognition for both DNA strands. Comput Chem 1993;17:123–33. https://doi.org/10.1016/0097-8485(93)85004-V.

[22] Kelley DR, Liu B, Delcher AL, Pop M, Salzberg SL. Gene prediction with Glimmer for metagenomic sequences augmented by classification and clustering. Nucleic Acids Res 2012;40(1):e9. https://doi.org/10.1093/nar/gkr1067.

[23] Buchan DWA, Jones DT. The PSIPRED protein analysis Workbench: 20 years on. Nucleic Acids Res 2019;47(W1):W402–7. https://doi.org/10.1093/nar/gkz297.

[24] Kyte J, Doolittle RF. A simple method for displaying the hydropathic character of a protein. J Mol Biol 1982;157(1):105–32. https://doi.org/10.1016/0022-2836(82)90515-0.

[25] De Santi C, Altermark B, de Pascale D, Willassen NP. Bioprospecting around Arctic islands: marine bacteria as rich source of biocatalysts. J Basic Microbiol 2016;56(3):238–53. https://doi.org/10.1002/jobm.201500505.

[26] Hyatt D, Chen GL, Locascio PF, Land ML, Larimer FW, Hauser LJ. Prodigal: prokaryotic gene recognition and translation initiation site identification. BMC Bioinform 2010;11:119. https://doi.org/10.1186/1471-2105-11-119.

[27] Altschul SF, Gish W, Miller W, Myers EW, Lipman DJ. Basic local alignment search tool. J Mol Biol 1990;215(3):403–10. https://doi.org/10.1016/S0022-2836(05)80360-2.

[28] Jia K, Cao R, Hua DH, Li P. Study of class I and class III polyhydroxyalkanoate (PHA) synthases with substrates containing a modified side chain.

Biomacromolecules 2016;17(4):1477–85. https://doi.org/10.1021/acs.biomac.6b00082.
[29] Buckley RM, Stubbe J. Chemistry with an artificial primer of polyhydroxybutyrate synthase suggests a mechanism for chain termination. Biochemistry 2015;54(12):2117–25. https://doi.org/10.1021/bi501405b.
[30] Schrader JM, Zhou B, Li GW, Lasker K, Childers WS, Williams B, et al. The coding and noncoding architecture of the *Caulobacter crescentus* genome. PLoS Genet 2014;10(7):e1004463. https://doi.org/10.1371/journal.pgen.1004463.
[31] Yuan W, Jia Y, Tian J, Snell KD, Muh U, Sinskey AJ, et al. Class I and III polyhydroxyalkanoate synthases from *Ralstonia eutropha* and *Allochromatium vinosum*: characterization and substrate specificity studies. Arch Biochem Biophys 2001;394(1):87–98. https://doi.org/10.1006/abbi.2001.2522.
[32] Gerngross TU, Snell KD, Peoples OP, Sinskey AJ, Csuhai E, Masamune S, et al. Overexpression and purification of the soluble polyhydroxyalkanoate synthase from *Alcaligenes eutrophus*: evidence for a required posttranslational modification for catalytic activity. Biochemistry 1994;33(31):9311–20. https://doi.org/10.1021/bi00197a035.
[33] Zhang S, Yasuo T, Lenz RW, Goodwin S. Kinetic and mechanistic characterization of the polyhydroxybutyrate synthase from *Ralstonia eutropha*. Biomacromolecules 2000;1(2):244–51. https://doi.org/10.1021/bm005513c.
[34] Pfeiffer D, Jendrossek D. PhaM is the physiological activator of poly(3-hydroxybutyrate) (PHB) synthase (PhaC1) in *Ralstonia eutropha*. Appl Environ Microbiol 2014;80(2):555–63. https://doi.org/10.1128/AEM.02935-13.
[35] Higuchi-Takeuchi M, Motoda Y, Kigawa T, Numata K. Class I polyhydroxyalkanoate synthase from the purple photosynthetic bacterium *Rhodovulum sulfidophilum* predominantly exists as a functional dimer in the absence of a substrate. ACS Omega 2017;2(8):5071–8. https://doi.org/10.1021/acsomega.7b00667.
[36] Mezzolla V, D'Urso OF, Poltronieri P. Role of PhaC type I and type II enzymes during PHA biosynthesis. Polymers 2018;10(8). https://doi.org/10.3390/polym10080910.
[37] Lim H, Chuah JA, Chek MF, Tan HT, Hakoshima T, Sudesh K. Identification of regions affecting enzyme activity, substrate binding, dimer stabilization and polyhydroxyalkanoate (PHA) granule morphology in the PHA synthase of *Aquitalea* sp. USM4. Int J Biol Macromol 2021;186:414–23. https://doi.org/10.1016/j.ijbiomac.2021.07.041.
[38] Kim YJ, Choi SY, Kim J, Jin KS, Lee SY, Kim KJ. Structure and function of the N-terminal domain of *Ralstonia eutropha* polyhydroxyalkanoate synthase, and the proposed structure and mechanisms of the whole enzyme. Biotechnol J 2017;12(1). https://doi.org/10.1002/biot.201600649.
[39] Jergic S, Ozawa K, Williams NK, Su XC, Scott DD, Hamdan SM, et al. The unstructured C-terminus of the tau subunit of *Escherichia coli* DNA polymerase III holoenzyme is the site of interaction with the alpha subunit. Nucleic Acids Res 2007;35(9):2813–24. https://doi.org/10.1093/nar/gkm079.
[40] Christensen M, Jablonski P, Altermark B, Irgum K, Hansen H. High natural PHA production from acetate in *Cobetia* sp. MC34 and *Cobetia marina* DSM 4741(T) and in silico analyses of the genus specific PhaC2 polymerase variant. Microb Cell Fact 2021;20(1):225. https://doi.org/10.1186/s12934-021-01713-0.
[41] Georlette D, Blaise V, Collins T, D'Amico S, Gratia E, Hoyoux A, et al. Some like it cold: biocatalysis at low temperatures. FEMS Microbiol Rev 2004;28(1):25–42. https://doi.org/10.1016/j.femsre.2003.07.003.
[42] Collins T, Gerday C. Enzyme catalysis in psychrophiles. In: Margesin R, editor. Psychrophiles. Cham: Springer; 2017. p. 209–35.
[43] Sheu DS, Chen WM, Lai YW, Chang RC. Mutations derived from the thermophilic polyhydroxyalkanoate synthase PhaC enhance the thermostability and activity of PhaC from *Cupriavidus necator* H16. J Bacteriol 2012;194(10):2620–9. https://doi.org/10.1128/JB.06543-11.
[44] Assefa NG, Niiranen L, Willassen NP, Smalas A, Moe E. Thermal unfolding studies of cold adapted uracil-DNA N-glycosylase (UNG) from Atlantic cod (*Gadus morhua*). A comparative study with human UNG. Comp Biochem Physiol B Biochem Mol Biol 2012;161(1):60–8. https://doi.org/10.1016/j.cbpb.2011.09.007.
[45] Sinha S, Surolia A. Oligomerization endows enormous stability to soybean agglutinin: a comparison of the stability of monomer and tetramer of soybean agglutinin. Biophys J 2005;88(6):4243–51. https://doi.org/10.1529/biophysj.105.061309.
[46] Chanasit W, Hodgson B, Sudesh K, Umsakul K. Efficient production of polyhydroxyalkanoates (PHAs) from *Pseudomonas mendocina* PSU using a biodiesel liquid waste (BLW) as the sole carbon source. Biosci Biotechnol Biochem 2016;80(7):1440–50. https://doi.org/10.1080/09168451.2016.1158628.
[47] Favaro L, Basaglia M, Casella S. Improving polyhydroxyalkanoate production from inexpensive carbon sources by genetic approaches: a review. Biofuels Bioprod Bioref 2019;13:208–27. https://doi.org/10.1002/bbb.1944.
[48] Silva JA, Tobella LM, Becerra J, Godoy F, Martinez MA. Biosynthesis of poly-beta-hydroxyalkanoate by B*revundimonas vesicularis* LMG P-23615 and *Sphingopyxis macrogoltabida* LMG 17324 using acid-hydrolyzed sawdust as carbon source. J Biosci Bioeng 2007;103(6):542–6. https://doi.org/10.1263/jbb.103.542.
[49] Obruca S, Dvorak P, Sedlacek P, Koller M, Sedlar K, Pernicova I, et al. Polyhydroxyalkanoates synthesis by halophiles and thermophiles: towards sustainable production of microbial bioplastics. Biotechnol Adv 2022:107906. https://doi.org/10.1016/j.biotechadv.2022.107906.